

## The $\omega$ Phase Formation during Laser Cladding and Remelting of Quasicrystal Forming AlCuFe on Pure Aluminum

Krishanu Biswas<sup>1</sup>, Kamanio Chattopadhyay<sup>1</sup>, Rolf Galun<sup>2</sup> and Barry L. Mordike<sup>2</sup>  
<sup>1</sup>Department of Metallurgy, Indian Institute of Science, Bangalore-560012, India  
<sup>2</sup>IWW, Technical University, Clausthal, Clausthal-Zellerfeld, D-38678, Germany

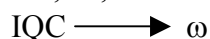
### ABSTRACT

We report the formation of  $\omega$  phase in the remelted layers during laser cladding and remelting of quasicrystal forming Al<sub>65</sub>Cu<sub>23.3</sub>Fe<sub>11.7</sub> alloy on pure aluminum. The  $\omega$  phase is absent in the clad layers. In the remelted layer, the phase nucleates at the periphery of the primary icosahedral phase particles. A large number of  $\omega$  phase particles forms enveloping the icosahedral phase growing into aluminum rich melt, which solidify as  $\alpha$ -Al solid solution. On the other side it develops an interface with aluminum. A detailed transmission electron microscopic analysis shows that  $\omega$  phase exhibits orientation relationship with icosahedral phase. The composition analysis performed using energy dispersive x-ray analyzer suggests that this phase has composition higher aluminum than the icosahedral phase. The analysis of the available phase diagram information indicates that the present results represent large departure from equilibrium conditions. A possible scenario of the evolution of the  $\omega$  phase has been suggested.

### INTRODUCTION

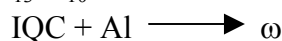
The icosahedral quasicrystal (IQC) of compositions around Al<sub>62.5</sub>Cu<sub>25</sub>Fe<sub>12.5</sub> was first reported by Tsai et al. [1]. Many authors have investigated Al-Cu-Fe ternary phase diagram depicting the solidification pathways [2-8]. The solidification of alloys of composition close to the canonical quasicrystalline phase Al<sub>62.5</sub>Cu<sub>25</sub>Fe<sub>12.5</sub> is quite complex and involves a large number of complex crystalline phases, like monoclinic Al<sub>13</sub>Fe<sub>4</sub> ( $\lambda$ , space group C2/m, a=1.5489 nm, b=0.80831 nm, c=1.2476 nm,  $\beta$ =107.72°), orthorhombic Al<sub>23</sub>CuFe<sub>4</sub> or Al<sub>6</sub>Fe ( $\tau_1$ , space group Cmc2<sub>1</sub>, a=0.744 nm, b=0.6464 nm, c=0.8779 nm), tetragonal Al<sub>7</sub>Cu<sub>2</sub>Fe ( $\omega$ , space group P4/mnc, a=0.6336 nm, c=1.481 nm) and cubic AlFe ( $\beta$ , space group Pm3m, a=0.2909 nm). Icosahedral phase has equilibrium phase field with these phases at higher temperature (>600°C). The studies on phase equilibria in the ternary icosahedral phase forming Al-Cu-Fe system suggest a series of possible pathways for  $\omega$  phase formation involving peritectic reactions [2-5].

There are few reports about formation of  $\omega$  phase during solid-state transformation of IQC. Köster et al [9-10] have reported that  $\omega$  phase forms by two ways during solid state heat treatment. In the first case, the polymorphic transformation of the IQC in melt-spun Al<sub>70</sub>Cu<sub>20</sub>Fe<sub>10</sub> alloy leads to formation of  $\omega$  phase, i.e.,



The  $\omega$  phase crystallites preferably nucleate at the IQC phase boundaries, but also inside the IQC phase during this polymorphic transformation.

In the second case, IQC transforms to  $\omega$  phase by a peritectoid reaction during isothermal annealing of melt-spun Al<sub>77</sub>Cu<sub>13</sub>Fe<sub>10</sub>



In this case the  $\omega$  crystallites nucleate at IQC/ $\alpha$ -Al interfaces and grow preferably along them so that IQC becomes encircled by the  $\omega$  crystallites. Further transformation proceeds by advancement of the  $\omega$ /IQC interface towards IQC. Grushko et al. [7] have reported the formation of  $\omega$  phase in slowly solidified sample (between 1000 and 500°C) in case of  $\text{Al}_{58.5}\text{Cu}_{35.5}\text{Fe}_6$  alloy. They have also found that the  $\omega$  phase crystallites surround the primary IQC. Rosas et al. [11] have also reported a structural transformation of IQC to  $\omega$  by peritectoid reaction similar to Köster et al. during annealing of  $\text{Al}_{72}\text{Cu}_{27}\text{Fe}_5$  alloy at 700°C. In this paper we report transmission electron microscopic study of  $\omega$  phase formation during laser cladding and remelting of  $\text{Al}_{65}\text{Cu}_{23.3}\text{Fe}_{11.7}$  on pure aluminum. The morphology, structure as well as solidification behavior of  $\omega$  phase have been discussed.

## EXPERIMENTAL DETAILS

Clads were prepared using  $\text{CO}_2$  laser with power level of 5 kW. The diameter of the laser beam was 5 mm. The powder feed rate used was 2 gm/min. and the flow rate of the carrier gas maintained was six liter per minute. The laser track width was 2 mm. The laser beam used was of multimode configuration. An argon jet was used to shield the melt pool from oxygen. The substrates were moved under the stationary laser beam by a numerically- controlled X-Y table. The nominal chemical composition of powder mixture  $\text{Al}_{65}\text{Cu}_{23.3}\text{Fe}_{11.7}$  was obtained by mechanically mixing commercially pure elemental powder (99% minimum) of Al, Cu and Fe. The particle size of powders was between 25 to 100  $\mu\text{m}$ . The powder mixture was carried by an argon jet, through a nozzle with inner diameter of 2 mm and delivered to the melt pool. The substrate used for deposition of coatings was pure aluminum (99.9%) and was sand blasted prior to the cladding experiments in order to clean the surface and obtain uniform roughness. The coatings were prepared by using the two-step cladding process. The optimized scan rate for cladding was 300 mm/min at laser power of 5 kW. The subsequent remelting experiments were carried out by employing scan rates at 300, 500 and 1000 and 1200 mm/min. Characterization of remelted layers has been performed using transmission electron microscope (JEOL make 2000FXII). The local phase composition was determined in TEM by standardless energy-dispersive x-ray analyzer (EDS), supplied by Oxford Instruments.

## RESULTS

The morphology and phase structure of the  $\omega$  phase is shown in figure 1. Fig. 1a shows bright field micrograph revealing the nucleation of  $\omega$  phase along the periphery of primary spherical IQC. One can find that a large number of  $\omega$  particles forming along the periphery of the IQC. The figure 1b shows the growth of  $\omega$  along the boundary of one such IQC particle. The inset (bottom) shows typical five- fold diffraction pattern taken from the IQC phase. The  $\omega$  grains form a rim long IQC phase. It develops an interface with aluminum. Micro-diffraction pattern taken along [011] zone axis from one such aluminum grain is shown in the inset (top). The series of micro-diffraction patterns taken from  $\omega$  phase is shown in fig 1c-e. The micro-diffraction pattern along [001] zone axis indicates the presence of superlattice spots of {100} type. Therefore,  $\omega$  phase has ordered tetragonal lattice. The results of composition analysis of the IQC and the  $\omega$  phase are shown separately in table 1. It can be seen that  $\omega$  contains more aluminum and less copper than IQC although the iron content remaining almost same. In order to study

whether there exists any orientation relationship between  $\omega$  and IQC, the icosahedral phase is oriented along two-fold direction. The  $\omega$  phase particles, which are in contact with IQC, are oriented to the nearest possible zone axis. The results are shown in fig. 2. Figure 2a shows the

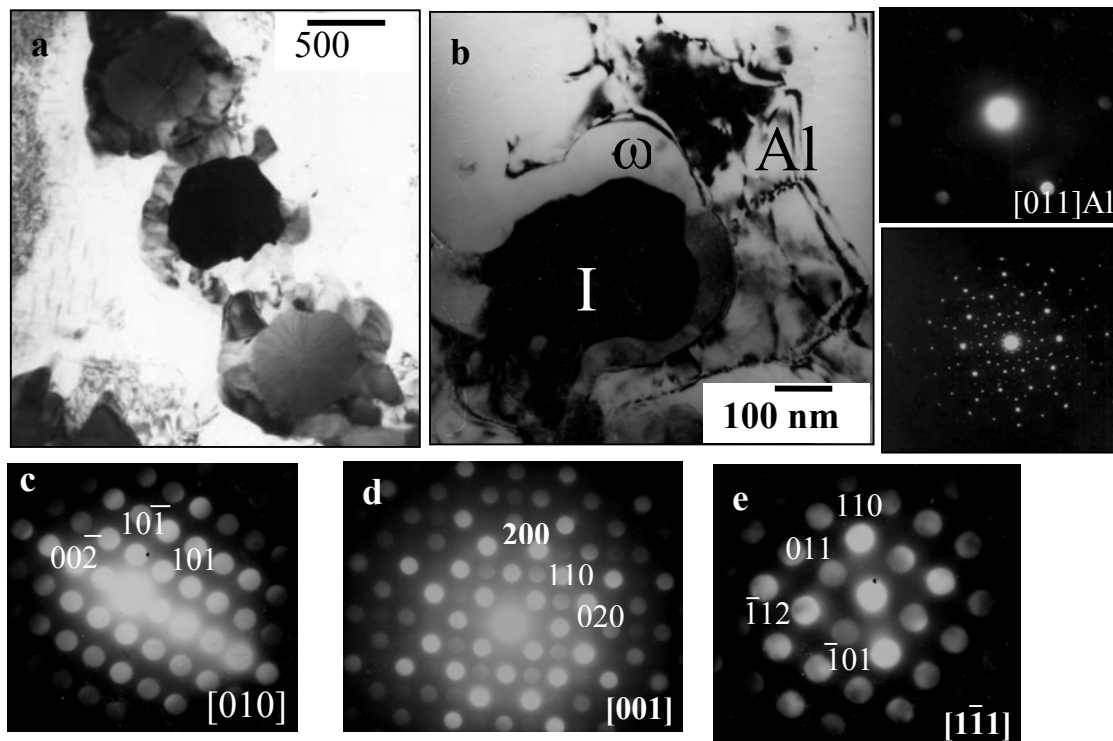


Figure 1: (a) Typical bright field micrograph showing  $\omega$  phase particles growing at the interface of the central icosahedral particle, (b) high magnification bright field image of one such icosahedral particle surrounded by  $\omega$  particles. Inset (bottom): SADP taken from icosahedral phase showing typical five fold symmetry and (top): micro-diffraction pattern along [011] zone axis of the aluminum and (c), (d) & (e) micro-diffraction patterns taken from  $\omega$  particles.

Table1: The elemental composition of IQC and  $\omega$  phase determined by EDS.

Phases	Al (at%)	Cu (at%)	Fe (at%)
IQC	<b>64</b>	<b>25.5</b>	<b>10.5</b>
$\omega$ -phase	<b>71</b>	<b>19.5</b>	<b>9.5</b>

bright field micrograph showing that five  $\omega$  grains growing along the periphery of a central icosahedral particle. The  $\omega$  grains are marked as 1 to 5. The typical 2-fold pattern taken from the icosahedral phase is shown in fig. 2b. We have taken micro-diffraction patterns from all the  $\omega$  grains. It has been found that  $\omega$  grains are oriented along [001] direction. But the diffraction patterns taken from grains 1, 2 and 5 and grains 3,4 along [001] axis are oriented differently. This is a clear indication that  $\omega$  phase is growing with different variants. It can be seen that all the  $\omega$  phase particles are oriented along [001] zone axis. Another important feature of growth of

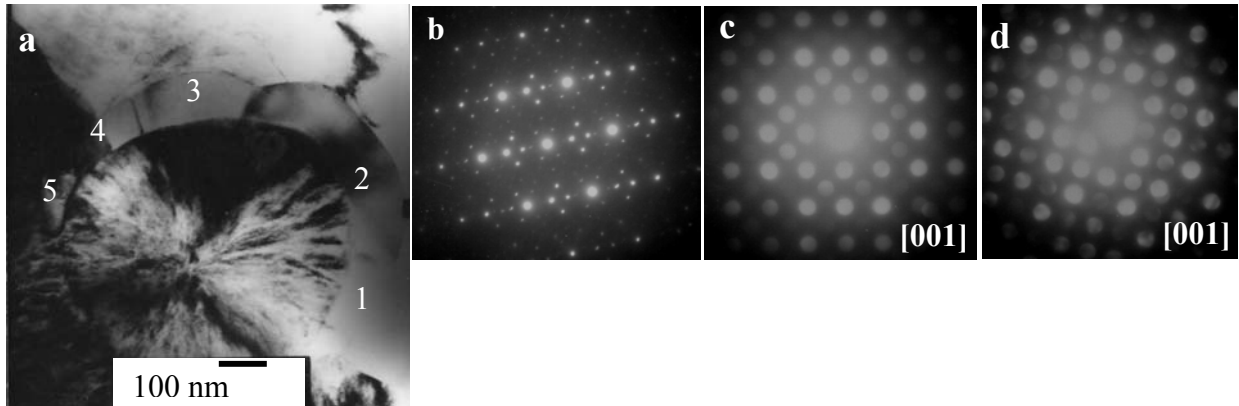


Figure 2: (a) Bright field micrograph showing icosahedral phase with  $\omega$  phase forming along the periphery of the icosahedral phase, (b) 2-fold zone axis of the icosahedral phase, (c) micro-diffraction taken along [001] from  $\omega$  grains 1,2,5 and (d) micro-diffraction taken along [001] from  $\omega$  grains 3,4.

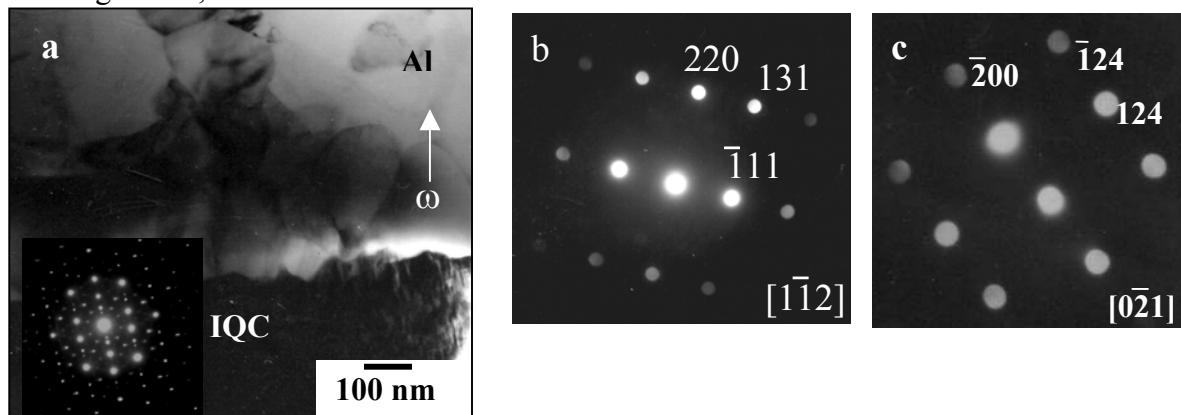


Figure 3: (a) Bright field micrograph showing the growth of  $\omega$  grains into the aluminum grains with bottom inset showing pseudo-five fold zone axis pattern IQC, (b)  $[1\bar{1}2]$  zone axis pattern of aluminum and (c)  $[0\bar{2}1]$  zone axis pattern of  $\omega$ .

$\omega$  phase is shown in figure 3. Figure 3a shows the bright field image showing  $\omega$  grains growing away from the icosahedral phase. The inset shows the pseudo five fold pattern taken from the icosahedral phase. The figure 3b shows micro-diffraction pattern taken from aluminum along  $[1\bar{1}2]$  zone axis. The micro-diffraction pattern taken from one of the  $\omega$  phase particles is shown in fig. 3c. This is a clear indication that  $\omega$  phase has grown into aluminum grains.

## DISCUSSION

The microstructure evolution of as clad  $\text{Al}_{65}\text{Cu}_{23.3}\text{Fe}_{11.7}$  alloy on pure aluminum was discussed in an earlier paper [14]. In the as-clad condition the amount of quasicrystalline phase was limited. In contrast, amount of quasicrystalline phase is significantly larger in the remelted layer. Most of these quasicrystals in the remelted layers are surrounded by another phase. The

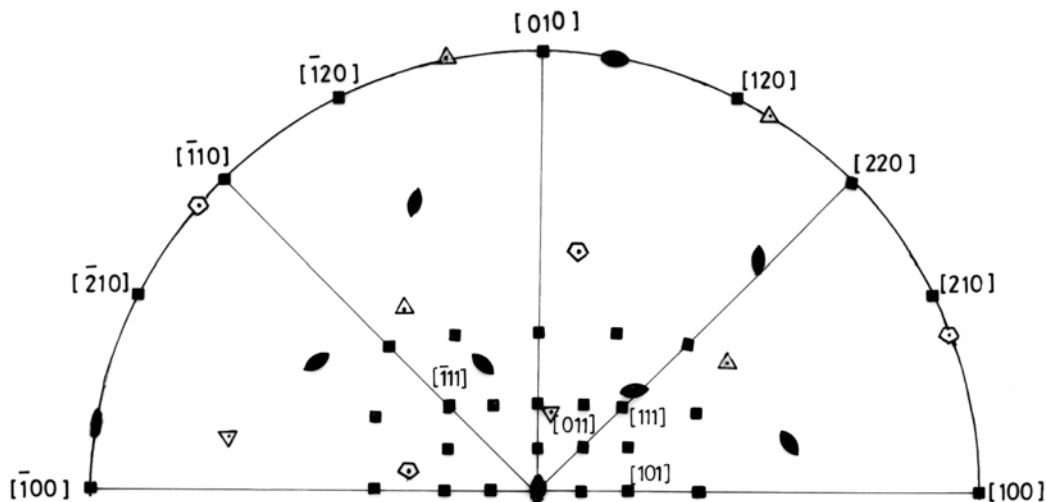


Figure 4: The half of stereogram showing the orientation-relationship between IQC and  $\omega$  [001]

electron diffraction patterns establish this phase to be the  $\omega$  phase with an ordered tetragonal structure. The observed lattice parameters are  $a = 0.6336$  nm and  $c = 1.487$  nm. Careful tilting experiments establish that this phase has an orientation relation with quasicrystal grain it surrounds as shown in fig.4. The two-fold zone axis of the quasicrystalline phase is parallel to the 001 zone axis of the tetragonal phase. The two-fold direction of the quasicrystal in the reciprocal space is 10 degree away from the 100 direction of the tetragonal plane. This clearly indicates that the  $\omega$  phase nucleates on the two fold planes of the quasicrystal. There are 16 distinct two fold directions (out of 32 directions), which can be parallel to 001 zone axis of the  $\omega$  phase. Since two planes of  $\omega$  phase, (100) and (010), which can align at an angle with each two fold direction of quasicrystal in the reciprocal space, one expect 32 distinct variants of  $\omega$  phase that can form. The two variants associated with a given two-fold zone can clearly be seen in figure 2. Thus, the crystallographic observations suggest heterogeneous nucleation of  $\omega$  phase on quasicrystal.

The detailed phase evolution and solidification pathways are first discussed by Gayle et al. [2]. Recently a very detailed and rigorous investigation on the ternary phase equilibria has been carried out by Zhang et al. [3-5]. We shall aim at understanding the observed results in the light of this series of papers. In the discussion of the phase evolution we shall only concentrate on the remelted region where  $\omega$  has been found to form. This phase could not be observed in the as clad conditions. Taking the nominal alloy composition,  $\text{Al}_{65}\text{Cu}_{23.3}\text{Fe}_{11.7}$  the appearance of phases as the alloy cools from the liquid state can be arrived from the isopleths. This is given below

$$L \rightarrow L+\lambda \rightarrow L+\lambda+\text{IQC} \rightarrow L+\text{IQC} \rightarrow \text{IQC} \rightarrow \text{IQC} + \omega$$

The applicability of this sequence to our situation encounters two difficulties. The laser cladding and in particular, remelting will take the system out of equilibrium due to higher cooling rates. Probably a more serious difficulty is the dilution of the composition due to mass transport from the substrate resulting in development of composition gradient in the remelted region.

Experimentally, we observe in addition to IQC and  $\omega$  phase, significant amount of  $\alpha$ -Al and  $\theta$  phase in the remelted region adjacent to the clad layer. The morphologies of phases clearly suggest direct nucleation of IQC phase in aluminum rich melt in this layer. The  $\lambda$ -phase, which has been predominantly found in the clad layer, reappeared only in the top section of the remelted layer with a finer length scale. Clearly, the dilution by aluminum during remelting played a significant role in the microstructure development in addition to the kinetic undercooling imposed by high rate of heat transfer. For the nominal composition  $\text{Al}_{65}\text{Cu}_{23.3}\text{Fe}_{11.7}$ ,

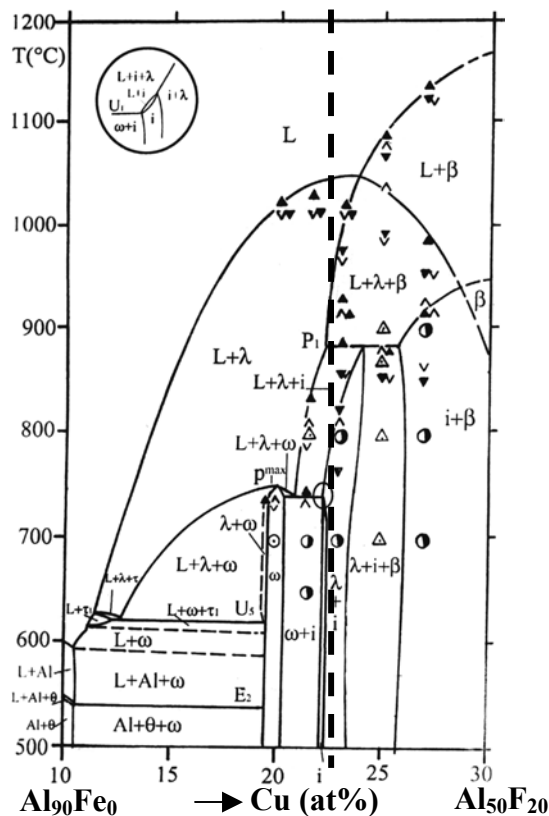


Figure 5: Isopleth along the  $\omega$ -IQC tie line (a compositional line between  $\text{Al}_{90}\text{Cu}_{10}$  and  $\text{Al}_{50}\text{Cu}_{30}\text{Fe}_{20}$  where the ratio  $(X_{\text{Cu}} - 10)/X_{\text{Fe}} = 1$  [4]. This diagram is used to explain possible solidification pathways for evolution of  $\omega$  phase in the remelted layer. The dotted line indicates the nominal composition of the alloy.

phase equilibria given by Zhang et al. [3-5], demand an undercooling of about  $150^\circ\text{C}$  for finite driving force for nucleation of the IQC phase. This can be seen in figure 5 drawn after Zhang et al. [4]. With dilution of aluminum, the phase field will most likely shift towards  $(\omega + \text{IQC})$  phase field resulting in heterogeneous nucleation of  $\omega$  on IQC in a non-equilibrium manner forming metastable coupled eutectic of  $\alpha$ -Al and  $\theta$  phases.

In order to further understand the evolution of the  $\omega$  phase, one needs to determine whether this phase is a product of peritectoid or peritectic reaction or the phase forms by a simple precipitation from the undercooled liquid. During solid-state heat treatment the peritectoid reaction was experimentally established in an earlier study [9-10]. However, the time scale of this experiment was much longer. There are reports [3,7] in the literature that  $\omega$  phase formation occurs by a peritectic reaction between liquid and IQC. Zhang et al. [3] has shown presence of clear DTA (Differential Thermal Analysis) peak due to the formation of the  $\omega$  phase from liquid at a temperature of  $667^\circ\text{C}$  when the  $\text{Al}_{62}\text{Cu}_{34.5}\text{Fe}_{3.5}$  sample is cooled from liquid state at a rate of  $10\text{K}/\text{min}$ . One-way to ascertain whether the  $\omega$  phase is a reaction product or not is to examine the nature of the interfaces that it has with quasicrystal and aluminum. As can be seen from the morphology in fig.4 (marked by the arrow), the  $\omega$  phase grows into the aluminum matrix. Further, the interface between the  $\omega$  phase and the quasicrystal is sharp in all microstructures

shown. Both these observations rule out a reaction between the aluminum (in liquid or solid state) and the quasicrystal. The  $\omega$  phase most likely nucleates on the two fold planes of quasicrystals and grows outward. In fact, it is possible to calculate the time needed for the growth of  $\omega$  of typical thickness observed in our microstructure (300nm) using a model of diffusion-controlled growth [12]. The diffusivity in liquid is typically  $10^{-8}\text{m}^2\cdot\text{s}^{-1}$ . The time needed to form the observed thickness of  $\sim 300\text{nm}$  is of the order of  $10^{-5}$  s. The measured solid-state diffusivity of Fe in IQC at  $\sim 550\text{-}600^\circ\text{C}$  (the temperature range of the peritectoid reaction [9]) is of the order of  $10^{-16}\text{m}^2\cdot\text{s}^{-1}$ [13]. Assuming that all the species have similar diffusivity, the time needed for the growth of the  $\omega$  phase layer in solid state at this temperature range is of the order of the order of  $\sim 10^3$  s. Recently we have estimated the temperature fields of the laser surface alloyed pools of Al-Ni alloy on the Ni substrate. The initial cooling rate after solidification is fairly high (of the order of  $10^3$  to  $10^4\text{K/s}$ ). For our case the substrate is aluminum and the cooling rate in the solid state is expected to be similar. Thus it is unlikely that the transformation observed in our sample has taken place in the solid state. Since the interface does not suggest any peritectic reaction, we conclude that the  $\omega$  phase precipitates on quasicrystal by a heterogeneous nucleation mechanism and grows into the aluminum rich melt till the super saturation is exhausted.

## CONCLUSIONS

We have observed formation of  $\omega$  phase in the remelted of  $\text{Al}_{65}\text{Cu}_{23.3}\text{Fe}_{11.7}$  which has been deposited on aluminum substrate by laser cladding. The results of a detailed characterization suggest that  $\omega$  phase in our sample nucleates heterogeneously on quasicrystalline phase, which has formed directly in the melt during resolidification. The phase is shown to grow into the aluminum rich melt. The sequence suggests microstructure evolution through a non-equilibrium solidification pathway for the remelted layer.

## REFERENCES

- [1] A.P.Tsai, A.Inoue and T.Masumoto, *Jpn.J.Appl.Phys.* 26. L1505. 1987
- [2] F.W.Gayle, A.J.Shapiro, F.S.Biancaniello and W.J.Boettinger, *Met. Trans.* 23A. 2409. 1992
- [3] L.Zhang and R.Lück, *Z.Metallkd.*, 94. 91. 2003
- [4] L.Zhang and R.Lück, *Z.Metallkd.*, 94. 98. 2003
- [5] L.Zhang and R.Lück, *Z.Metallkd.*, 94. 108. 2003
- [6] D.Gratias, Y.Calvayrac, J.Devaud-Rzepski, F.Faudot, M.Harmelin, A.Quivy and P.A.Bancel, *J.Non-Cryst.Solids*, 153&154. 482. 1993
- [7] B.Gruskho, R.Wittenberg and D.Holland-Moritz, *J.Mater.Res.*, 11(9). 2177. 1996
- [8] J.Gui, J.Wang, R.Wang, D.Wang, J.Liu and F.Chen, *J.Mater.Res.*, 16(4). 1037. 2001
- [9] W.Liu and U. Köster, *Mater. Sc. and Engg.* A133. 338. 1991
- [10] U. Köster and W.Liu, *Phase Transitions*, 44. 137. 1993
- [11] G.Rosas and R.Perez, *Materials Lett.*, 47. 225. 2001
- [12] H.B.Aaron, D.Fainstein and G.E.Kotler, *J. App.Phys.*, 41 (11). 4404. 1970
- [13] J. -L. Joulaud, J.Bernardini, P.Gas, C.Bergman, J.-M.Dubois, Y.Calvayrac and D.Gratias, *Phil Mag. A.* 75 (5). 1287. 1997
- [14] K. Biswas, R.Galun, B.L.Mordike and K.Chattopadhyay, *J. Non-Cryst. Solids as Proc. of ICQ8*, ed. S.Ranganathan and K.Chattopadhyay and K.F.Kelton, Bangalore. 2002. in press